MEASUREMENT OF CYCLOTRON BEAM PHASE SPACE

V. S. PANDIT, P. R. SARMA, R. K. BHANDARI

Variable Energy Cyclotron Centre

1/AF Bidhan Nagar, Calcutta-700 064, India

The experimental determination of particle beam emittance and density distribution in the transverse and longitudinal phase spaces have been discussed. These methods are applicable to beams with any kind of density distribution in the phase space. Analysis of the longitudinal phase space data clearly shows the decomposition of the beam into three components. The orientation of the phase ellipse indicates a marginal improvement in the time resolution with the energy analysis of the beam.

1 Introduction

The beam from an Azimuthally Varying Field (AVF) cyclotron consists of short pulses arriving at the frequency of the rf oscillator. The quality of the beam consisting of identical charged particles is generally defined by its two transverse emittances (relating position and divergence) and one longitudinal emittance (relating energy resolution and time structure). The basic aim associated with the design and optimization of the accelerator parameters is to have beams with low phase space area in all the three planes and intensity as high as possible. In general, the points in the phase space are denser near the origin and the area occupied by 90% of the points may be several times that occupied by half of them. Under these circumstances, the area of the phase space which determines the emittance is not well defined. For this reason, it is necessary that the beam phase space density distribution be measured to evaluate the emittance. A prior knowledge of the density distribution of the particles in the phase spaces and orientation of the phase ellipses helps in efficient transport of the beam and estimation of the beam quality downstream in the beam line.

In the present work we have calculated the values of rms transverse emittance by developing a simple formula which relates the measured rms widths of the profile to the rms spatial and angular widths of the beam. We have also calculated the values of the longitudinal emittance as a function of the beam percentage and compared the result with the theory curve based on gaussian distribution. We have studied the dependence of emittance on various machine parameters.

2 Transverse Emittance

There are various experimental techniques available to measure the transverse emittance and have been discussed in detail in ref.[1]. A simple and nondestructive method is the "three gradient method" in which one uses a quadrupole lens and a beam profile monitor. In this, one measures the beam profile for three different settings of quadrupole current and then uses the transport matrix and the beam matrix to calculate the emittance. This method measures the emittance and gives the orientation of phase ellipses. It does not give any indication about the distribution of particles in the phase space. We have developed a simple formula to evaluate the rms emittance which is valid for any kind of spatial and angular distributions of particles in the phase space [2]. We have related the width of the profile to the spatial and angular distributions of the beam and have used this dependence to calculate the emittance.

Let us consider a section of the beam line in which a quadrupole is separated from a downstream beam profile monitor (BPM) by a field free drift space L. The relation between the density distribution function at the quadrupole (ρ) and at the BPM

(ρ_1) is given by

$$\rho_1(x,\theta) = \rho\left[(x - L\theta), \{\theta(1-\frac{L}{F}) + \frac{x}{F}\}\right] \qquad (1)$$

where F is the focal length of the quadrupole. The rms width of the beam at the BPM can be related to the rms width of the profile at the quadrupole by

$$< x_1^2 >= \left[1 - \frac{L}{F}\right]^2 < x^2 > +L^2 < \theta^2 >$$

$$+ 2L\left[1 - \frac{L}{F}\right] < x\theta > \qquad (2)$$

This equation gives the rms spacial width of the beam at the BPM which is valid for any kind of profile distribution of the beam. One can easily evaluate $< x_1^2 >$ for various settings of the quadrupole current and hence the required parameters to calculate rms emittance given by

$$\epsilon_{rms} = 4(< x^2 >< \theta^2 > - < x\theta >^2)^{\frac{1}{2}} \qquad (3)$$

The three beam lines of our laboratory are each equipped with a rotating wire type beam profile monitor (model BPM6 of NEC make). A digital storage oscilloscope coupled to an IBM PC was used to record the beam profile. Beam transport parameters were set to obtain the beam waist near the BPM and a series of profile measurements were taken by varying the strength of the quadrupole magnet. Care was taken to see that these measurements cover a range of quadrupole strength with mean around the strength corresponding to the waist.

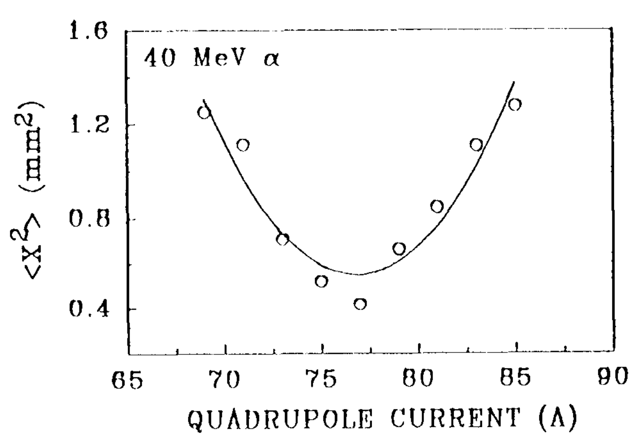

Figure 1: Variation of the measured $< x^2 >$ of the beam profile as a function of the current in the quadrupole. The full curve is the least-squares fit to the data.

Figure 1 shows the variation of the mean square width $< x^2 >$ of beam profile as a function of the current in the quadrupole magnet which focuses the beam in the horizontal plane. Open circles represent the measured data points. A least square fit (the full curve) was used to get the required parameters. We obtained a value of the rms emittance equal to 6.32±.44 mm.mrad.

We have also studied the effect of beam current on the emittance. Emittance measurements were carried out using 30 MeV alpha beam at 1.0mA, 1.5mA, 2.0mA and 2.5mA. All the parameters of the cyclotron were kept fixed during the experiment. Beam current was changed by changing the arc current of the ion source. We observed that emittance is only weakly dependent on the beam current as shown in figure 2.

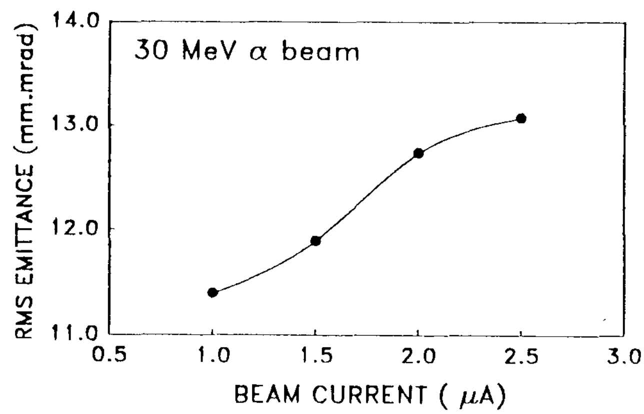

Figure 2: The variation of the rms emittance with the beam current.

3 Longitudinal emittance

Measurements of the longitudinal phase space of the cyclotron beam have been carried out by Ettinger et.al [3]. Their method is based on measuring the waveform of the beam current at three different places, using a probe and bending magnets. Another method based on time of flight analysis of protons scattered from a thin carbon fibre has been used by Th. Stammbach [4] to improve the longitudinal phase space of internal cyclotron beam. Our method [5] is based on a simple experiment where elastically scattered projectile particles from a thin target are detected in coincidence with the rf signal i.e., the time profile of the beam itself. We have used a typical elastic scattering experiment such as $^{197}Au(\alpha,\alpha)$. A gold target having a thickness of

$400\mu g/cm^2$ and a home made surface barrier detector with energy resolution of $50keV$ and placed at forward angle of 17^0 were used in the experiment. The energy and time spectra were recorded in two ADC in a two parameter list mode block by block (one block was defined as 4096 events) on a disk file using a PC based data acquisition system developed at the centre.

Fig.3 shows the longitudinal phase space obtained by displaying the $2D$-spectra after gating the time ADC with the elastic alpha energy peak and energy ADC with the alpha-rf time structure peak. The area of the phase space is $28.2 \times 10^{-3} eVs$ (electron volt second) and consists of approximately 90% of the particles. It appears from the phase plot that the points are dense near the origin, and the isodensity contours form a set of closed curves, roughly elliptical in shape. The orientation of the phase ellipse is clearly visible indicating a correlation between time and energy. The FWHM of the energy distribution is $320keV$ and that of the time is $10ns$.

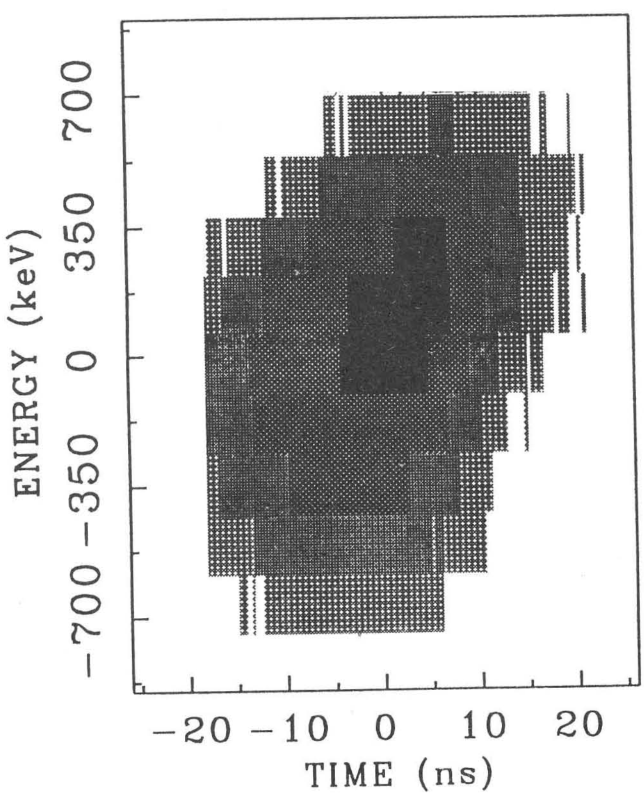

Figure 3: Longitudinal phase space in t, E co-ordinates for $40MeV$ alpha beam. Density of the points is maximum at the center and the change of intensity between the equidensity contours (represented by different shades) is by a factor of 7.

Fig.4 shows the dependence of longitudinal emittance on the beam percentage together with the theoretical curve based on the gaussian distribution. The difference between the two curves indicates that the experimentally measured density distribution of the beam in the phase space deviates slightly from the gaussian distribution.

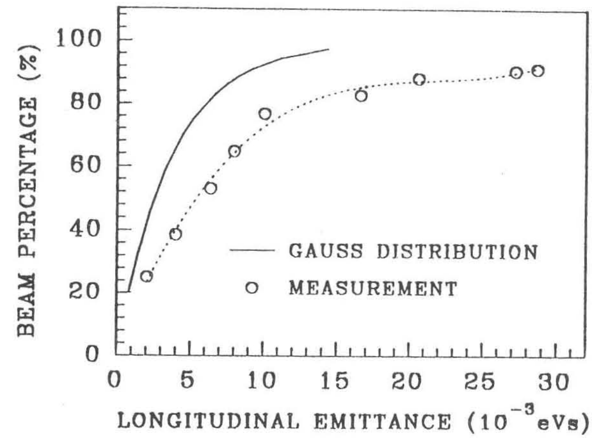

Figure 4: Dependence of longitudinal emittance on beam percentage obtained experimentally together with the theory curve based on gaussian distribution

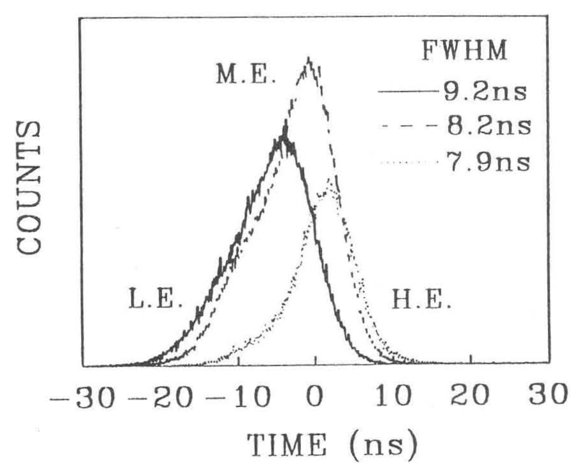

Figure 5: Decomposition of beam pulse into three components obtained by setting three equal energy gates each of $200keV$ on the elastic peak starting from the low energy side in the energy ADC and projecting the time spectrum from list mode data.

The beam from the cyclotron reveals a complex structure in longitudinal phase space. The FWFM of the elastic peak is around $600keV$ which is three times the energy gain per turn (dee voltage was $50kV$). In order to find out the time distribution of these three components of the beam, three equal gates of $200keV$ each were set on the elastic peak in the energy ADC begining from the lower energy side and the alpha-rf time spectra on the time ADC were projected from the list mode data. These time projections are shown in Fig.5. The decomposition of the beam pulse into three components is clearly visible. The leading and the lagging edges of the beam are formed of the faster and the slower particles respectively and the shift in the time peaks from the mean position is around $2.6ns$ for each component. This indicates a phase lag between the successive turns at extraction radii. We believe that this type of structure of the beam originates from multiturn extraction due to overlapping of neighbouring orbits near the extraction radii.

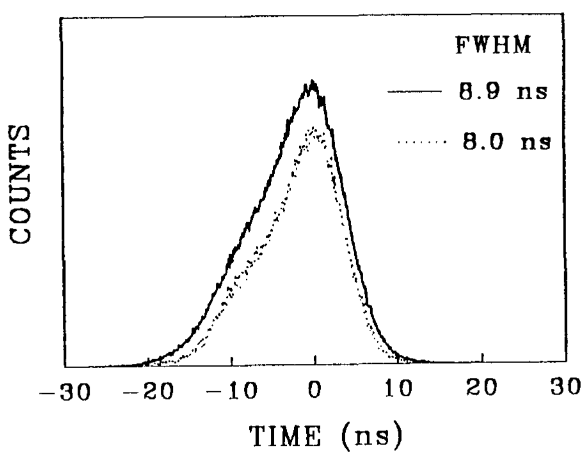

Figure 6: Time spectrum of the beam obtained by setting two energy gates of $600keV$ (solid curve) and $90keV$ (dotted curve) on the elastic peak in the energy ADC and projecting the time ADC.

Results of the study of beam time distribution when an energy window is selected are shown in Fig.6. Here we have set two gates of $600keV$ and $90keV$ on the energy ADC and projected the time ADC from list mode data. As it appears from Fig.6, the two distributions are essentially identical, but with slight reduction in FWHM. It remains the same when the energy window is reduced from $90keV$ to $50keV$. This behavior is expected also from the orientation of the phase ellipse shown in Fig.3. This study confirms that the energy selection of beam with the analysing magnet will not produce any significant improvement in the time spectrum of the beam.

4 Conclusion

We have presented a complete method of measuring the density distribution and the emittance in the phase space. Such an exercise will be helpful in estimating the beam properties downstream in the beam line and matching the longitudinal as well as the transverse phase space when a pulsed beam from one accelerator is injected to another one. It is to be noted that all the measurements are stochastic in nature and individual bunches are not recorded, and so the calculated values are the average values. We also point out that a detector with low energy resolution will give better results.

Acknowledgments. The authors acknowledge with thanks the help and support provided by Dr S. K. Basu, Mrs D. Bandyopadhyay, Mr Amitava Roy and Prof. P. Sen (SINP).

References

[1] A. Septier (Ed.);Applied Charged Particle Optics, Part A, Academic Press (1980).

[2] V.S. Pandit, P.R. Sarma, S. Bhattacharya and R. K. Bhandari; Meas. Sci. Technol **8** (1997) 1085.

[3] K.V. Ettinger, J.F.B. Dealler and F.R. Stewart; Proc. 5th Int. Cyclotron Conf. (Ed: R.W McIlory) Butterworths, London (1971) 333.

[4] Th. Stammbach, Proc. 13th Int. Conf. on Cyclotrons and Their Applications (Ed: G. Dutta and M.K. Craddock), World Scientific (1992) 28.

[5] V. S. Pandit; Nucl. Instr. and Meth. (1998) (in press).